Electrochemical and Photoelectrochemical Properties of New Hybrid Langmuir−Blodgett Films Containing Prussian Blue and a Tris(Bipyridine) Ruthenium Derivative

Gemma Romualdo Torres, Eliane Dupart, Christophe Mingotaud, and Serge Ravaine*

Centre de Recherche Paul Pascal, CNRS, Avenue A. Schweitzer, F-33600 Pessac, France

Received: April 4, 2000; In Final Form: June 30, 2000

The elaboration of new Langmuir−Blodgett (LB) films containing Prussian blue and a surfactant derivative of the ruthenium tris(bipyridine) complex using a semi-amphiphilic approach is described in this paper. The redox and photoelectrochemical properties of these hybrid lamellar materials have been studied in aqueous KCl solutions. Dependencies of the cyclic voltammetry response on the number of deposited layers and the scan rate demonstrate that the hybrid LB films can be considered as a quasireversible system with a finite diffusion space. A large cathodic photocurrent is recorded when the LB films are irradiated with polychromatic light at a negative applied potential, indicating that both PB and the derivative of ruthenium tris(bipyridine) complex play an important role in the light-energy conversion process. A linear dependence of the cathodic photocurrent response on the number of deposited layers has also been exhibited and should be correlated to the presence of structural defects in the multilayers.

Introduction

The design and synthesis of new hybrid organic/inorganic materials have attracted much attention in recent years.[1−4] The research has been motivated by the goal of developing novel functional materials, such as sensors or nonlinear optical devices, whose properties are superior to those of conventional materials. According to recent studies devoted to the elaboration of molecular magnetic materials,[5−6] the control at the molecular level of the spatial arrangement of both inorganic and organic parts of the hybrid systems is crucial to effectively combine their physicochemical properties.

It is well-known that the quantum efficiency of photoenergy conversion systems is greatly improved by controlling the molecular organization of photosensitizers and electroactive species to inhibit the back electron-transfer process. Therefore, many attempts to intercalate photosensitive compounds into various molecular assemblies such as micelles, microemulsions, electrodeposited films, and LB films have been made.[7−13] We have focused our attention on the elaboration of new hybrid multilayered materials containing electroactive species intercalated into layers of photosensitive molecules to produce new photofunctional systems. In this study, we report the formation of LB films comprising Prussian blue (PB) and a surfactant derivative of ruthenium tris(bipyridine) complex, using the semi-amphiphilic strategy.[14] Both the $Ru(bpy)_3^{2+}$ complex and PB have received much attention from the viewpoint of their application to various molecular devices.[15−17] For example, Kaneko et al. have reported that graphite electrodes were made photoresponsive by coating them with bilayer membranes of PB and polymer-pendant $Ru(bpy)_3^{2+}$.[18−19] We do expect that the original structure of the lamellar materials described in this paper enables a large photocurrent efficiency, as the photosensitizer and the electroactive species are very close.

Therefore, the redox and photoelectrochemical properties of the hybrid LB films deposited onto ITO (indium tin oxide) electrodes have been investigated in aqueous KCl solutions. The recorded cyclic voltammetry and photoelectrochemical behaviors suggest, indeed, that electron transport through the lamellar materials is efficient, probably because of the presence of structural defects.

Experimental Section

Reagents and Materials. Prussian blue and potassium chloride (99.9%) were purchased from Aldrich, and dimethyldioctadecylammonium bromide (DODA) (99%) from Kodak. The surfactant derivative of ruthenium tris(bipyridine) complex (**1**), $Ru(bpy)[bpy(C_{17})_2]_2^{2+}$, where bpy = 2,2′-bipyridine and $C_{17} = (CH_2)_{16}CH_3$, was synthesized and purified according to the already published procedure.[20] The purity of **1** was verified by elemental analysis. Calculated (%): C, 68.37; H, 9.30; N, 4.88; Ru, 5.87; Cl, 4.12. Found (%): C, 66.75; H, 9.12; N, 5.03; Ru, 5.56; Cl, 4.73. ITO glass slides were obtained from ICMC (Le Mée-sur-Seine, France) and were cleaned by sequential sonication in acetone and distilled water prior to each experiment.

Procedures. Spreading solutions were prepared from HPLC-grade chloroform (Prolabo) and were kept at −18 °C between experiments to limit solvent evaporation. An appropriate amount of a solution of **1** was carefully spread onto water or a 10^{-5} M Prussian blue aqueous solution such that the initial area per molecule was close to 250 Å^2, and the spreading solvent was allowed to evaporate for 10 min prior to compression. The Langmuir monolayers were compressed at 20 ± 1 °C using a step-by-step procedure. The Y-type **1**/PB LB films were obtained by the vertical lifting method with a transfer ratio close to unity, at a target pressure of 30 mN/m with a dipping speed of 1 cm/min. After each cycle, the substrate was allowed to dry for 5 min in nitrogen. The Y-type DODA/PB LB films were elaborated as previously reported.[5]

Instrumentation. The LB experiments were carried out with a laboratory-made trough.[21] Surface pressure was measured with a platinum Wilhelmy plate. A Millipore purification system produced water with a resistivity higher than 18 MΩ cm for all experiments. All of the electrochemical experiments were carried

* To whom correspondence should be addressed.

10.1021/jp0013006 CCC: $19.00
Published on Web 09/15/2000

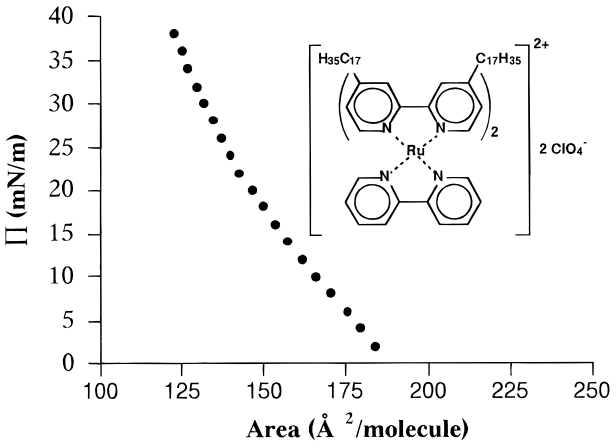

Figure 1. Surface pressure−area isotherm of **1** on water.

out in a three-electrode conventional cell at the ambient laboratory temperature (20 ± 1 °C) in KCl aqueous solutions that had been bubbled with nitrogen for at least 20 min. The cyclic voltammetry and photoelectrochemical experiments were conducted with an Autolab PGSTAT 20 potentiostat from EcoChemie, computer-controlled by their General Purpose Electrochemical System. Potentials were measured with respect to a saturated calomel electrode (SCE). UV−visible spectra were recorded with an Unicam UV 4 spectrophotometer. For all of the photoelectrochemical experiments except the recording of the photocurrent action spectrum, the LB films were irradiated with white light from a KL 1500 halogen lamp (Schott, 150 W). The distance between the lamp and the electrode was about 1 cm. For the recording of the photocurrent action spectrum, light irradiation was made by a xenon lamp (65 W). Monochromatic light was obtained using a MS257 spectrograph from Oriel Instruments. The light intensity was measured with a photovoltaic detector (Oriel Instruments). The electrochemical and photoelectrochemical data were obtained for three LB films fabricated independently.

Results and Discussion

Monolayer Behavior and Multilayer Properties. Compound **1** spread at the gas/water interface forms a monolayer perfectly stable versus time. The corresponding Π−*A* isotherm shown in Figure 1 presents no kink or plateau, suggesting that the monolayer undergoes no phase transition during the compression. The isotherm starts from ca. 190 Å^2/molecule and shows a collapse at ca. 120 Å^2/molecule for a surface pressure around 40 mN/m. These values are quite comparable to those already published.[20] Contrary to other positively charged molecules, Prussian blue dissolved in the subphase does not strongly modify the compression isotherm. Indeed, the recorded variation in the area for a given surface pressure is less than 10% when the concentration of Prussian blue is increased up to 10^{-5} M. Transfer (Y-type) onto a hydrophobic substrate is easily performed at 30 mN/m with a transfer ratio close to unity. Infrared spectra demonstrate that Prussian blue is indeed trapped inside the LB structure. X-ray diffraction experiments show that at least some parts of this hybrid material have a lamellar structure with a periodicity of 36 Å.

Cyclic Voltammetry. The redox properties of **1**/PB LB films deposited onto ITO electrodes were measured by cyclic voltammetry (CV). The voltammograms of films with 1, 3, 5, and 8 layers of PB in 0.50 M KCl aqueous solutions are shown in Figure 2. The three characteristic sets of reversible peaks corresponding to the metal-based Ru^{2+}/Ru^{3+} redox reaction

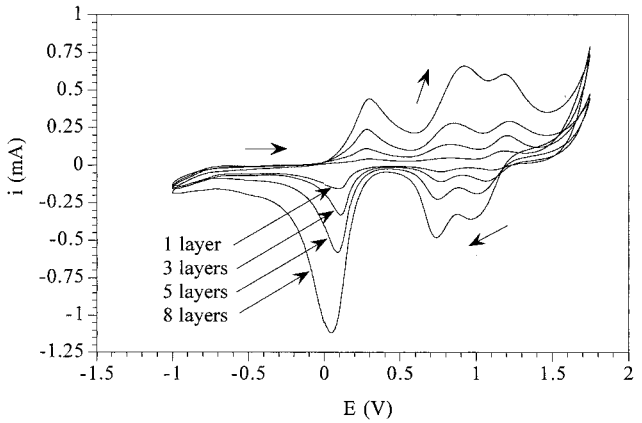

Figure 2. Cyclic voltammograms of **1**/PB LB films with 1, 3, 5, and 8 layers of PB in aqueous 0.5 M KCl. Scan rate = 0.5 V/s. Area of the electrode ≈ 1 cm^2. Starting point of scan: 0 V/SCE.

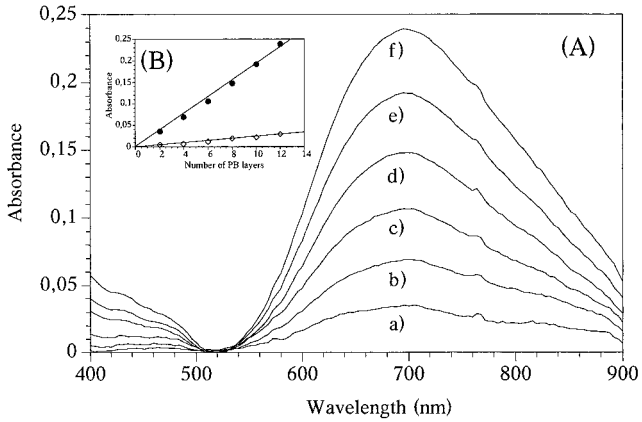

Figure 3. (A) Absorbance spectra of **1**/PB LB films with (a) 2, (b) 4, (c) 6, (d) 8, (e) 10, and (f) 12 layers of PB. (B) Dependence of the absorbances of **1**/PB LB films at (●) 700 and (◊) 460 nm on the number of PB layers.

(around 1.10 V),[22,23] the reduction of PB to Everitt's salt (around 0.2 V), and its oxidation to Prussian yellow (around 0.9 V) are clearly observed. All of the redox peaks increase with the number of deposited layers, indicating that both PB and **1** are homogeneously transferred during the LB film elaboration. This feature was confirmed by the UV−visible spectra of the lamellar systems (see Figure 3 A), as the intensity of both the characteristic absorption band of PB at 700 nm and the metal-to-ligand charge-transfer band of $Ru(bpy)_3^{2+}$ at 460 nm[24] increased linearly with the number of deposited layers (see inset 3B). The absorbance per layer at 460 nm, *D*, calculated from the slope in the linear relationship, is found to be 1.2×10^{-3} au/layer. From the Beer−Lambert law modified for two-dimensional concentration, i.e., $\Gamma = 10^{-3}D/\epsilon$, where Γ is the surface concentration (mol/cm^2) and ϵ is the molar absorption coefficient [ϵ = 14 000 L mol^{-1} cm^{-1} for $Ru(bpy)_3^{2+}$ [24]], the surface concentration of $Ru(bpy)_3^{2+}$ in the LB films is calculated to be 0.9×10^{-10} mol/cm^2. This value is smaller than the one estimated from the Π−*A* isotherm of **1** on 10^{-5} M PB aqueous solution (ca. 1.2×10^{-10} mol/cm^2). This difference may be due to a modification of the ϵ value of the $Ru(bpy)_3^{2+}$ complex in the multilayered systems and/or to the presence of structural defects in the organic layers, which probably arose during the transfer onto the ITO substrate.

Both the peak-to-peak separation and the half-peak widths increase with the thickness of the LB films. Such behavior has already been observed with similar hybrid lamellar systems[25]

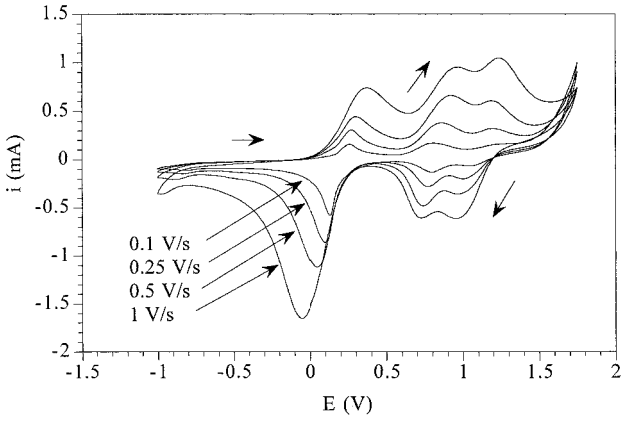

Figure 4. Dependence of the cyclic voltammogram of a **1**/PB LB film with 8 layers of PB on the scan rate. Supporting electrolyte: 0.5 M KCl. Area of the electrode ≈ 1 cm^2. Starting point of scan: 0 V/SCE.

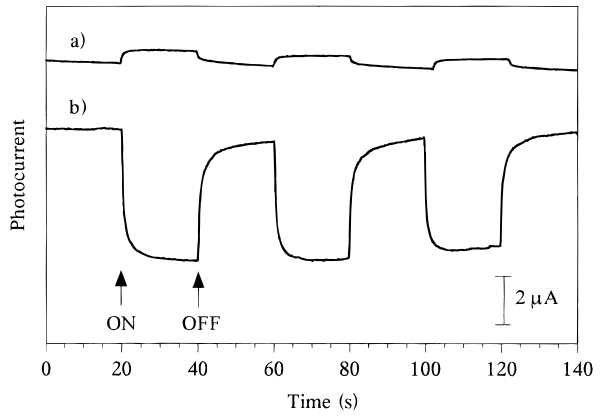

Figure 5. Current changes induced by switching on and off the irradiation of a **1**/PB LB film with 8 layers of PB. Supporting electrolyte: 0.5 M KCl. Applied potential = (a) 1 and (b) −0.5 V vs SCE. Area of the electrode ≈ 1 cm^2.

and has been correlated with the partial hindrance of the diffusion of the charged species through the multilayered materials by the increasing number of long-chain surfactant layers. Nevertheless, these films should present some structural defects to partially explain the observed electron transfer from the outer layers of the LB films to the ITO electrode.

The electrochemical behavior of the **1**/PB lamellar systems has been further investigated by recording the CV curves at different scan rates. Figure 4 shows, as an example, the dependence of the voltammogram of a LB film containing 8 layers of PB on the sweep rate. One can note that both the half-peak widths and the peak-to-peak separation increase with the scan rate. Meanwhile, the plot of the peak current versus the square root of the sweep rate exhibits a linear behavior (not shown). All of these results must be correlated with a large diffusion effect due to the presence of the 15 insulating long-chain surfactant layers.[26,27]

Photoelectrochemistry. As PB and the $Ru(bpy)_3^{2+}$ complex are a well-known redox reagent and a photosensitizer with a strong absorption around visible light, respectively, we investigated the light-energy conversion properties of the **1**/PB LB films. Figure 5 shows the photoresponses of a lamellar system containing 8 layers of PB under visible light irradiation at an applied potential of (a) +1and (b) −0.5 V. A stable photocurrent is induced reversibly by switching on and off the irradiation. Its direction is dependent on the applied potential. As shown in Figure 6, an applied potential higher than ca. 0.1 V vs SCE induced an anodic photocurrent and potentials lower than this

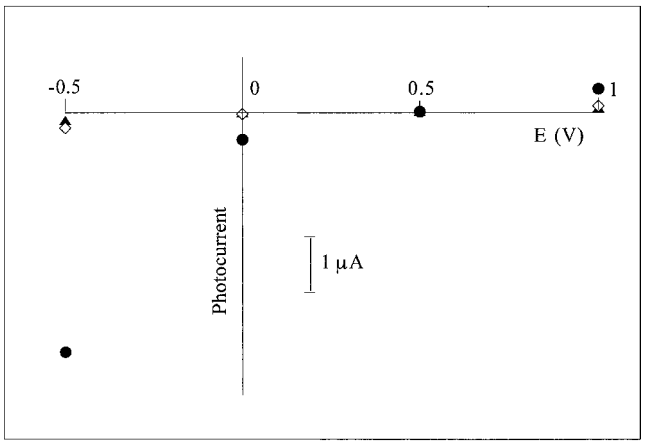

Figure 6. Dependence of the photocurrents of (●) a **1**/PB LB film with 8 layers of PB, (▲) a DODA/PB LB films with 8 layers of PB, and (◊) a LB film of 15 layers of **1** deposited from a pure water subphase on the applied potential. Supporting electrolyte: 0.5 M KCl. Area of the electrode ≈ 1 cm^2.

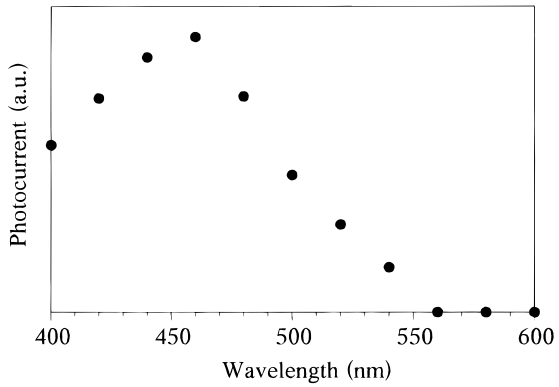

Figure 7. Photocurrent action spectrum of a **1**/PB LB films with 8 layers of PB. Supporting electrolyte: 0.5 M KCl. Applied potential = −0.5 V vs SCE. The photocurrent was normalized to the number of incident photons.

value a cathodic photocurrent. It can be seen that a significantly large cathodic photocurrent is obtained when a negative potential is applied, suggesting the p-type character of the hybrid LB films.

To determine the mechanisms of light conversion for the cathodic and anodic photocurrents, we compared the photoelectrochemical responses of **1**/PB LB films at various applied potentials with those registered under similar conditions for DODA/LB films and for LB films of **1** deposited from a pure water subphase. The results are shown in Figure 6. Only a small cathodic photocurrent on the order of tens of nanoamperes per square centimeter is induced by irradiating either LB films of **1** or the DODA/PB LB films when a negative potential is applied. This indicates that both the $Ru(bpy)_3^{2+}$ complex and PB play an important role in the cathodic photocurrent generation. The cathodic photocurrent of a **1**/PB LB films with 8 layers of PB was recorded as a function of irradiation wavelength (photocurrent action spectrum, Figure 7). The action spectrum shows a characteristic band around 460 nm, which corresponds to the metal-to-ligand charge-transfer band of $Ru(bpy)_3^{2+}$ in the absorption spectrum shown in Figure 3A. One can therefore suggest that the major mechanism of the cathodic photocurrent generation is based on the excitation of $Ru(bpy)_3^{2+}$. The resulting oxidative quenching of the excited Ru complex by PB is expected to be very efficient because these two entities are very close in the LB films. Such a result has been confirmed

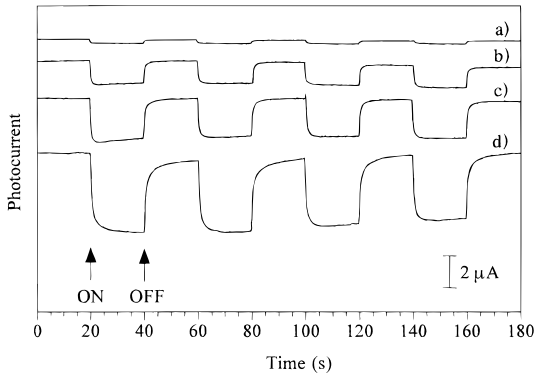

Figure 8. Current changes induced by switching on and off the irradiation of **1**/PB LB films with (a) 1, (b) 3, (c) 5, and (d) 8 layers of PB. Supporting electrolyte: 0.5 M KCl. Applied potential = −0.5 V vs SCE. Area of the electrode ≈ 1 cm^2.

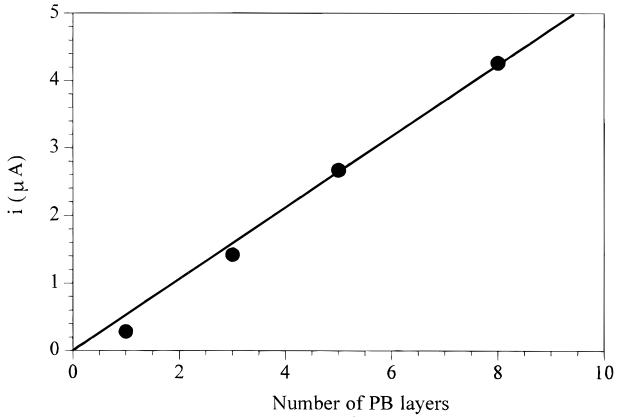

Figure 9. Dependence of the cathodic photocurrent at −0.5 V vs SCE of **1**/PB LB films on the number of PB layers.

by the emission spectra of **1**/PB LB films and LB films of **1**, which indicate that the response of the former is drastically reduced compared with that of the later.[28] The cathodic photocurrent is produced by a multistep electron transport from the ITO electrode through the lamellar materials. This charge transfer may be possible by an electron-hopping mechanism, but its exact course remains unclear. Moreover, the cathodic photoresponse of the **1**/PB LB films has found to be dependent on their thickness, as shown in Figure 8. The plot of the dependence of the photocurrent on the number of deposited layers exhibits a linear behavior (see Figure 9), which means that the multistep electron transport process is very efficient despite the presence of the insulating walls constituted by the alkyl chains grafted on the ruthenium tris(bipyridine) complex. This result is consistent with the observed electrochemical behavior of the **1**/PB LB films and should be correlated with the suggested presence of structural defects in the multilayers.[29]

As far as the anodic photocurrent is concerned, the association of PB and **1** does not seem to play a crucial role, as all three types of LB films give similar and small photocurrent responses when a positive potential is applied (see Figure 6). Considering the previously reported n-type character of the DODA/PB LB films,[30] one may suggest that the $Ru(bpy)_3^{2+}$ complex plays no role in the anodic photocurrent generation. A similar conclusion has been drawn by Kaneko et al. concerning bilayer membranes of polymer-pendant $Ru(bpy)_3^{2+}$ and PB.[18]

Conclusions

We have examined new hybrid LB films containing PB and a surfactant derivative of ruthenium tris(bipyridine) complex using a semi-amphiphilic approach. The electrochemical and photoelectrochemical properties of these lamellar systems have been studied in aqueous KCl solutions. A very large cathodic photocurrent is recorded when they are irradiated with polychromatic light at a negative applied potential. This photoelectrochemical behavior clearly results from the association at the molecular level of the organic and inorganic entities in the lamellar systems. This result supports our plan to design and build new hybrid materials whose properties are superior to those of conventional materials.

Acknowledgment. We thank Dr. L. Navailles for having performed the X-ray diffraction experiments and Dr. A. Dazzi for making the spectrograph available to us.

References and Notes

(1) Tamura, K.; Setsuda, H.; Tanigucha, M.; Yamagishi, A. *Langmuir* **1999**, *15*, 6915.
(2) Kleinfeld, E. R.; Ferguson, G. S. *Science* **1994**, *265*, 370.
(3) Kimizuka, N.; Handa, T.; Kunitake, T. *Mol. Cryst. Liq. Cryst.* **1996**, *277*, 189.
(4) Taguchi, Y.; Kimura, R.; Azumi, R.; Tachibana, H.; Koshizaki, N.; Shimomura, M.; Momozawa, N.; Sakai, H.; Abe, M.; Matsumoto, M. *Langmuir* **1998**, *14*, 6550.
(5) Mingotaud, C.; Lafuente, C.; Amiell, J.; Delhaes, P. *Langmuir* **1999**, *15*, 289.
(6) Einaga, Y.; Sato, O.; Iyoda, T.; Fujishima, A.; Hashimoto, K. *J. Am. Chem. Soc.* **1999**, *121*, 3745.
(7) Kaneko, M.; Yamada, A.; Tsuchida, E.; Kurimura, Y. *J. Phys. Chem.* **1984**, *88*, 1061.
(8) Miyashita, T.; Murakata, T.; Yamaguchi, Y.; Matsuda, M. *J. Phys. Chem.* **1985**, *89*, 497.
(9) Downard, A. J.; Surridge, N. A.; Gould, S.; Meyer, T. J.; Deronzier, A.; Moutet, J.-C. *J. Phys. Chem.* **1990**, *94*, 6754.
(10) Aoki, A.; Abe, Y.; Miyashita, T. *Langmuir* **1999**, *15*, 1463.
(11) Taniguchi, T.; Fukasawa, Y.; Miyashita, T.*J. Phys. Chem. B* **1999**, *103*, 1920.
(12) Wu, D.-G.; Huang, C.-H.; Gan, L.-B.; Zheng, J.; Huang, Y.-Y.; Zhang, W. *Langmuir* **1999**, *15*, 7276.
(13) Aoki, A.; Miyashita, T. *J. Electroanal. Chem.* **1999**, *473*, 125.
(14) Clemente-Leon, M.; Mingotaud, C.; Agricole, B.; Gomez-Garcia, C. J.; Coronado, E.; Delhaes, P. *Angew. Chem., Int. Ed. Engl.* **1997**, *36*, 1114.
(15) Kaneko, M.; Moriya, S.; Yamada, A.; Yamamoto, H.; Oyama, N. *Electrochim. Acta* **1984**, *29*, 115.
(16) Kaneko, M.; Hara, S.; Yamada, A. *J. Electroanal. Chem.* **1985**, *194*, 165.
(17) Upadhyay, D. N.; Gomathi, H.; Prabhakara Rao, G. *J. Electroanal. Chem.* **1991**, *301*, 199.
(18) Kaneko, M. *J. Macromol. Sci., Pure Appl. Chem.* **1987**, *A24*, 357.
(19) Kaneko, M.; Yamada, A. *Electrochim. Acta* **1986**, *31*, 273.
(20) Valenty, S. J.; Behnken, D. E.; Gaines, G. L. *Inorg. Chem.* **1979**, *18*, 2160.
(21) Clemente-Leon, M.; Agricole, B.; Mingotaud, C.; Gomez-Garcia, C. J.; Coronado, E.; Delhaes, P. *Langmuir* **1997**, *13*, 2340.
(22) Winkler, K.; Costa, D. A.; Hayashi, A.; Balch, A. L. *J. Phys. Chem. B* **1998**, *102*, 9640.
(23) Forster, R. J.; Keyes, T. E. *J. Phys. Chem. B* **1998**, *102*, 10004.
(24) Juris, A.; Balzani, V.; Barigelletti, F.; Campagna, S.; Belser, P.; Von Zelewsky, A. *Coord. Chem. Rev.* **1988**, *84*, 85.
(25) Saliba, R.; Agricole, B.; Mingotaud, C.; Ravaine, S. *J. Phys. Chem. B* **1999**, *103*, 9712.
(26) Aoki, K.; Tokuda, K.; Matsuda, H. *J. Electroanal. Chem.* **1983**, *146*, 417.
(27) Aoki, K.; Tokuda, K.; Matsuda, H. *J. Electroanal. Chem.* **1984**, *160*, 33.
(28) Mingotaud, C. Centre de Recherche Paul Pascal, CNRS. Personal communication, 1999.
(29) Atomic force microscopy experiments are currently underway to visualize these structural defects.
(30) Ravaine, S.; Lafuente, C.; Mingotaud, C. *Langmuir* **1998**, *14*, 6347.